Efficient Aerodynamic System of Rear and Front Wings for an FSAE Car

A Siddharth Reddy[1], Atheeq Ur Rehman[1], Sathvik Shetty[1], Shashank Vivek, Gajanan[1*]

[1]*Department of Mechanical Engineering, RV College of Engineering®, Bengaluru*

Abstract

In the early 1980s, the motor sport industry came up with a new way of enhancing the performance without compromising on the efficiency through the concept of aerodynamics - generating very high down force thereby increasing traction, with no reduction in efficiency. Although motor sport industries are engaged in research on automotive aerodynamics, open literature on the same is limited. This research presents design and development of front and rear wings for an existing FSAE prototype which can generate a down force of 25 to 30 kgf i.e. 1/8 of the weight of the existing prototype at an average speed of 14 m/s increasing the cornering efficiency of the car. Based on motorsport racing aerodynamic requirements and constraints, a high lift to drag ratio aerofoil S1223 was selected. Simulations were carried out in ANSYS Fluent on aerofoil wings designed using SOLIDWORKS. At Reynolds number 1.84×10^5, a total down force of 34.8 kgf and a total drag force of 8.317 kgf was generated using simulation.

Keywords: Aerofoil - S1223, Multi-element wing, CFD analysis, FSAE prototype, Downforce, Drag-coefficient

1.0 Introduction

Over the past few decades, motorsport racing has evolved rapidly due to the intense competition amongst motorsport racing companies. Key design directions for the cars include reduction of weight, increase in engine power within the competition restrictions, and enhancing cornering performance by incorporating aerodynamic surfaces [1]. The main purpose for using aerodynamic devices in cars is to increase the down force experienced by the car to ensure greater traction between the tyres and the ground especially during cornering so that the car can approach the corner at greater speed. This needs to be achieved while ensuring that the drag contributed by these devices is at its minimum to mitigate the negative effects of engine losses in overcoming drag. There are different types of aerodynamic attachments such as wings (both front and rear), diffusers, Gurney flaps, end plates and active aerodynamic devices like spoilers, active rear wing and active grille shutter [2].

---

*Mail address: Gajanan, Assistant Professor, Dept. of Mechanical Engg.,
RV College of Engineering®, Bengaluru – 59
E-mail: gajanan@rvce.edu.in, Ph: 8867550078

Wings used in motorsport racing are synonymous with the ones used in airplanes, with the major difference being the wings used in motorsports use inverted airfoils. One of the key aspects of a motorsports wing is that it operates in high ground effect. Peters et al [3] carried out wind tunnel studies on NACA0012 and DHMTU airfoil in ground effect and reported that that L/D ratio is superior at low angles of attack. Kaviem and Chelven [4] carried out an experimental study on NACA4412 airfoil in ground effect and reported that the performance is superior for angles of attack 4^0 to 8^0.

Wordley and Sanders [5] based on the work on aerodynamic package of an FSAE race car presented the down force calculations along with the understanding of balancing of the aerodynamic forces provided by the front and rear wings. Dalhberg [6] introduced the concept of inverse airfoil design for FSAE car. Zhang and Zerihan [7] presented comprehensive study of double element wing and different configurations of the wings to provide high down force. Review of literature indicated that aerofoil design, manufacturing processes and simulation parameters are not comprehensively reported. The present work was focussed on design and development of front and rear wing for an existing FSAE prototype car.

2.0 Detail Design with Computations

Initially, design of an airfoil that should cater to the motorsport aerodynamic requirements was carried out. During the design phase, multiple airfoil designs were considered and the best suited was selected after considering the characteristics and simulations were carried out for the desired result. Final wing configuration on the prototype with respect to rule constraints and number of wing elements was designed. After finalising the airfoil configuration, the wing configuration which included placement, angle of attack and chord length was fixed based on simulation. This phase included structural designing of the mounting and attachment points of the wings to the prototype's chassis.

2.1 Geometry

Direct method of designing is a process in which airfoil shape is selected from a set of airfoil library for motorsport application which involves low Reynolds number high lift wings. Coefficient of lift to drag vs. angle of attack and coefficient of lift with angle of attack was compared for different airfoils. After comparison, S1223 was selected as the desired airfoil. The selected airfoil (Fig. 1) is a high lift airfoil and has the highest lift to drag ratio at low Reynolds number.
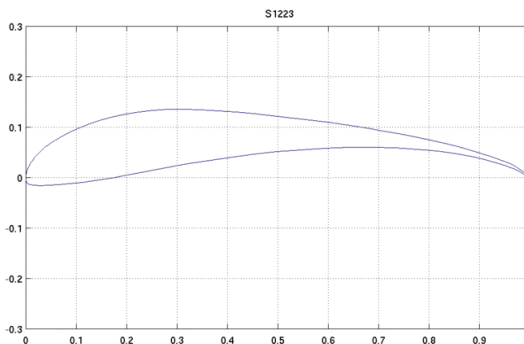
Fig. 1. S1223 Airfoil Geometry (scale: one unit is 0.1 unit length)

The operating velocity was chosen as 14 m/s which is the target speed of an FSAE prototype for entering a corner or a turn with the aerodynamic wings without losing traction at the wheels.

Calculation of Reynold's number:

$$Re = \frac{\rho V L}{\mu} \;\ldots\ldots\ldots\ldots\ldots\ldots\ldots.(1)$$

The fluid flowing is air

μ= Dynamic viscosity = 18.6 x 10^{-6} Pa s

ρ= Density of fluid = 1.225 kg/m^3

V= velocity = 14 m/s

L= Chord length of wing = 0.2 m

Re= $\frac{1.225*14*0.2}{18.6*10^{-6}}$ = 184408

The Reynolds number is within the limit of motorsport application and the chosen airfoil is suited for this.

For the overall wing assembly, the total downforce of 30kgf was kept as reference. S1223 airfoil of various chord lengths and various angle of attacks were used depending on the position of the elements of assembly were used to make the front wing and the rear wing.

For front wing, 3 segments with maximum of 2 elements were made to accommodate the wings as per FSAE rule book and rear wing was a 3-element assembly with the width complying the FSAE rulebook was designed. Fig. 2.a and 2.b shows the drawing of front and rear wing. Fig. 3 and 4 represents the Cad drawings of front and rear wing assembly respectively.
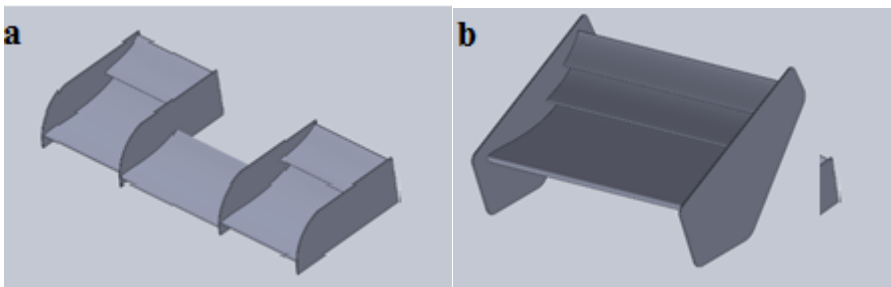
Fig. 2 a). Front Wing Assembly and **b).** Rear Wing Assembly
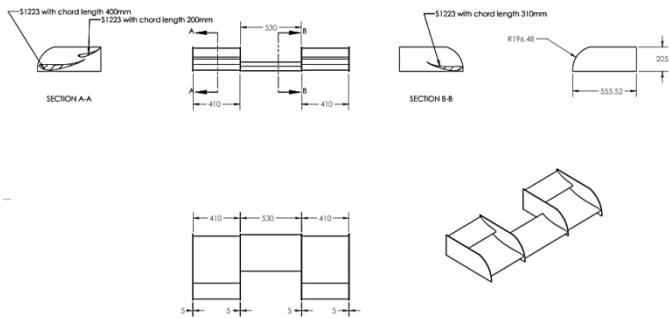
Fig. 3. Drawing of front wing
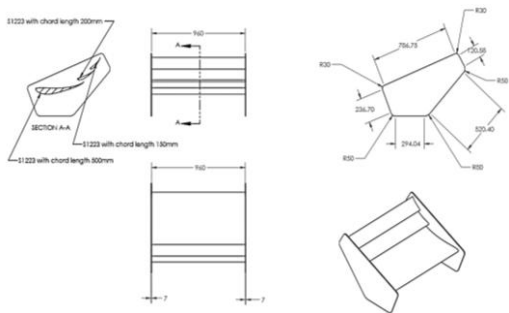
Fig. 4. Drawing of rear wing
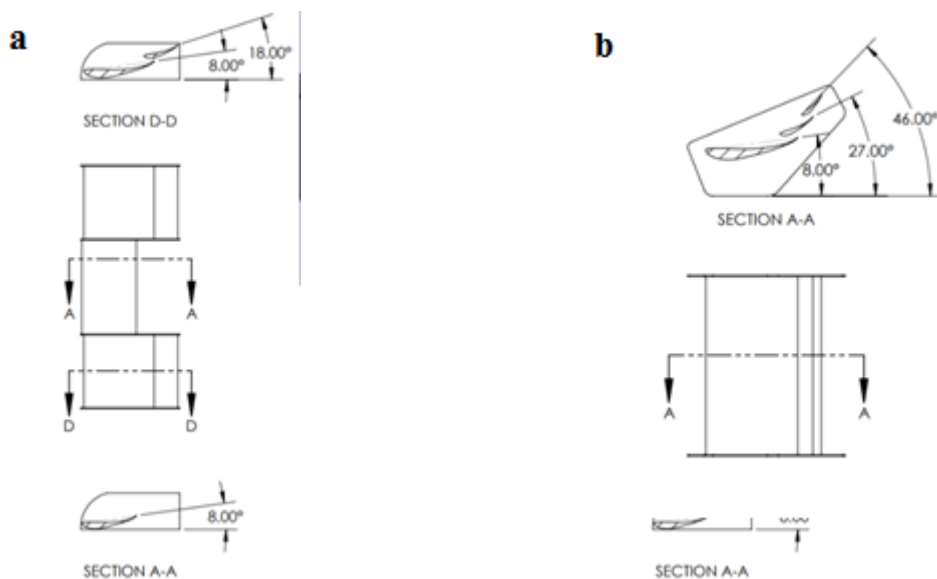
Fig. 5 a). Front wing Angle of Attack and **b).** Rear wing Angle of attack

Fig. 5.a and 5.b shows the angle of attacks for the two elements of front wing and three elements of the rear wing.

2.2 Meshing

Fig 6.a and Fig 6.b shows the mesh for the front wing and rear wing elements. Meshing was carried out in ANSYS Fluent meshing. For the mesh generation, a fine mesh setting was chosen. Further, inflation layer was added in order to capture boundary layer effects. Ten inflation layers were added by choosing a y+ factor of 1. The aspect ratio achieved for the front wing was 58.9 and that of the rear wing was 62.7 with a maximum skewness ratio of 0.958 for front wing and 0.907 for rear wing. These are within the limit of good mesh requirements of ANSYS Fluent. Table 1 shows the various meshing parameters and their corresponding values.
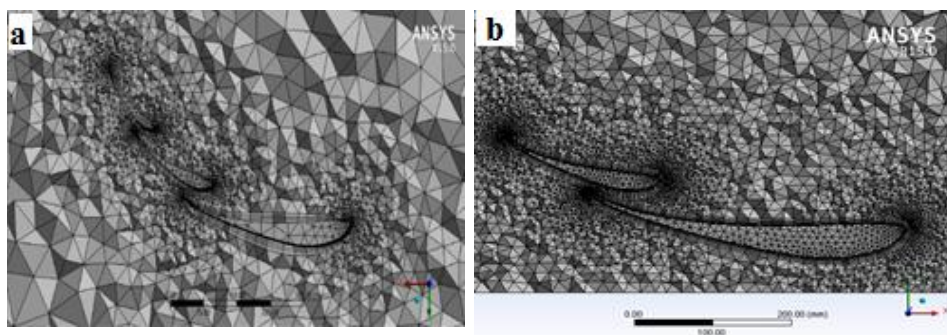
Fig. 6 a). Rear Wing Mesh and **b).** Front Wing Mesh

Table 1. Meshing parameters

Parameter	Value/Condition
Mesh sizing	Fine mesh
Y+	1
Number of Inflation Layers	10
Aspect Ratio – Front Wing	58.9
Aspect Ratio – Rear Wing	62.7
Skewness ratio – Front wing	0.958
Skewness ratio – Rear wing	0.907

2.3 Mesh independence test

The mesh independence test was performed with three different mesh sizes. The results are shown in Table 2 and table 3. The downforce and drag were considered as the variables which was used to determine if the mesh had converged. It is seen that the quantities vary considerably when comparing the coarse with medium mesh. However, there is no significant variation between the medium and fine meshes. Hence, the mesh with 5.2 million elements in the front wing and 6.2 million elements in the rear wing was considered for the study, as that was significantly faster to compute.

Table 2. Mesh independence study

Mesh elements			Downforce (N)		Drag (N)	
Front wing	Rear wing	Mesh type	Front wing	Rear wing	Front wing	Rear wing
3654889	4825974	Coarse mesh	155.2	169.4	25.9	42.5
5255694	6212394	Medium mesh	163.69	177.71	28.2	49.7
7845958	8745934	Fine mesh	163.91	177.96	28.5	49.9

Table 3. Percentage variation with mesh size

Mesh	Percentage variation			
	Downforce		Drag	
	Front wing	Rear wing	Front wing	Rear wing
Coarse and medium mesh	5.5%	4.9%	7.8%	14.4%
Medium and fine mesh	0.13%	0.14%	1.05%	0.4%

2.4 Analysis

The analysis was carried out on ANSYS Fluent. A steady state flow simulation was done as the car is not in acceleration condition and is considered as cruising condition. All the states of the dynamic system have reached the equilibrium levels. This means that the steady state values are the values that will be maintained as its after the time passed is tending to infinity. Table 4 depicts various analysis parameters chosen in Fluent.

For analysis, initially an enclosure was created around the wing assembly to simulate the surrounding environment.

Table 4. Analysis Parameters

Parameter	Value/condition
Viscous Model	K-Omega-SST
Solution method	COUPLED scheme
Initialization method	Hybrid initialization
Inlet Velocity	14 m/sec
Outlet Pressure	Zero Gauge Pressure
Condition for walls	No-slip and smooth

During analysis a velocity inlet, pressure outlet was chosen as those conditions are stable and are solvable. A velocity of 14m/s is chosen as that is a general cornering speed, and a zero-gauge pressure is chosen at the outlet. Further, a moving ground was chosen in order to capture ground effect for the front wing.

A viscous k-omega SST model is used for the simulation with curvature correction and production limiter as it captures the flow regime close to the wall as well as far away from it with the most accuracy. The SST model uses a mixing function value to automatically switch between k - ω (k-omega) and k - ε (k-epsilon) when close to or far away from a wall, respectively. The use of k - ω near the wall, where there would be boundary layer formation, makes the

model directly usable all the way down to the wall, including the viscous sublayer. Hence, the SST model can be used as a Low-Reynolds turbulence model as well. Switching to k - ε away from the wall avoids the common problem associated with k - ω, that is the high sensitivity of the model in free-stream regions to inlet free-stream turbulence properties. The below equations model the turbulence of flow according SST theory: Equation 1 takes care of the kinetic energy k of the fluid and the equation 2 gives rate of dissipation. Also, COUPLED scheme solution method was chosen as it is suitable for our requirement. A hybrid initialization was chosen as the solution initialization methods. The simulations were run until a residue value of 10^{-6} for mass and momentum.

$$\frac{\partial(\rho k)}{\partial t} + \frac{\partial(\rho u_j k)}{\partial x_j} = P - \beta^* \rho \omega k + \frac{\partial}{\partial x_j}\left[(\mu + \sigma_k \mu_t)\frac{\partial k}{\partial x_j}\right] \quad \ldots\ldots\ldots \quad (2)$$

$$\frac{\partial(\rho \omega)}{\partial t} + \frac{\partial(\rho u_j \omega)}{\partial x_j} = \frac{\gamma}{v_t}P - \beta\rho\omega^2 + \frac{\partial}{\partial x_j}\left[(\mu + \sigma_\omega \mu_t)\frac{\partial \omega}{\partial x_j}\right] + 2(1 - F_1)\frac{\rho\sigma_{\omega 2}}{\omega}\frac{\partial k}{\partial x_j}\frac{\partial \omega}{\partial x_j} \quad \ldots. (3)$$

Fig. 7 a and 7 b represents the static pressure and velocity contour around the rear wing. As it can be seen, the upper surface is at a higher pressure in comparison with the bottom surface, this pressure difference creates the down force required for increasing the traction
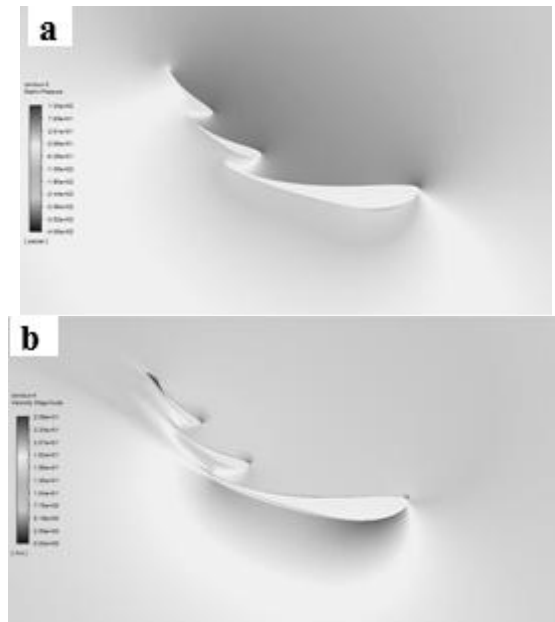
Fig. 7 a). Rear wing pressure contour and **b).** Rear wing velocity contour

3.0 Results

During the design phase, different aerofoils where considered initially with varying angle of attack and varying chord in order to achieve the desired downforce. Table 5 depicts the design methodology which is a highly iterative procedure. Multiple iterations were carried out to get to the final result. The simulations were carried out on ANSYS Fluent.

Table 5. Results of multiple iterations during design phase

Wing Elements		Angle of attack ($\square$, deg)		Chord Length (mm)		Downforce and Drag (N)	
Front Wing	Rear Wing	Front Wing	Rear Wing	Front Wing	Rear Wing mm	Front Wing	Rear Wing
NACA2415	FX74	5.5,7.5	8, 27,38	400, 250	400,250,200	108.4, 18.3	149.2,25.6
NACA2415	E423	5.5, 9	8, 27,38	450, 250	400,250,200	113.2,20.3	140.5,36.5
E423	E423	9,15	8,30,45	400,250	300,250,150	119.2,21.6	143.2,41.3
E423	E423	9, 15	8,30,39	400,275	350,250,150	121.2, 26.3	149.2,39.5
S1223	S1223	8, 15,	8, 28,43	400, 250	350,200,150	125.6, 35.6	147.3,47.3
S1223	S1223	8, 14,8	8, 30,45	400,250,310	350,250,150	123.5, 36.7	167.5,46.2
S1223	S1223	9, 15,8	9, 25,40	400,250,250	400,250,200	134.7, 32.4	160.4,43.5
S1223	S1223	8, 15,8	8, 27,40	310,200,200	400,250,150	141.5, 31.7	165.9,45.6
S1223	S1223	8, 18,8	8, 28,46	400,200,310	500,200,150	163.69,29.8	177.7,49.7

3.1. Front wing

Compared to the rear wing, the front wing is very close to the ground, which induces ground effect. This is caused primarily by the ground interrupting the wingtip vortices and downwash behind the wing. The simulations were run till the residual values reaches around 10^{-6}. Table 6 represents the report of drag force and down force for front wing obtained from ANSYS Fluent. It can be seen that a down force of 163.69 N and a drag of 29.84 N was developed on front wing

Table 6. Result report of down force and drag force from ANSYS Fluent

Zone	Down Force (N)	Drag Force (N)
Wall-enclosure	163.69685	29.835473
Net	163.69685	29.835473

Front wing was simulated first till the desired result is obtained and later moment balancing is performed to obtain the desired rear wing result. This is because, front wing design is heavily constrained by the rulebook and the number of wing elements that can be accommodated. And there are many ways

in which the downforce from rear wing can be changed with greater ease as there is more space and scope to make modifications on the rear wing.

The downforce from the front wing is 163.69N. Hence, by performing moment balancing between front and rear wing, the approximate downforce expected for the rear wing can be obtained. The moment balance was done by the following method as described below. Figure 8 shows the side view of the prototype with dimensions used for calculating the down force of rear wing.

1. The front edge of the front wing is at a distance 700mm from leading edge of the front wheel and COG is assumed to be in the middle, i.e. 350mm from leading edge of front tire.
2. The rear edge of the rear wing is at a distance 250mm from trailing edge of the rear wheel and COG is assumed to be in the middle, i.e. 125mm from leading edge of front tire.
3. Radius of tire is 225mm
4. COG of the whole prototype is at the middle of the wheelbase

The moment is balanced about the CoG as the force provided by the wings shouldn't affect the suspension characteristics of the vehicle as the changes in suspension characteristics may cause instabilty in vehicle performance.
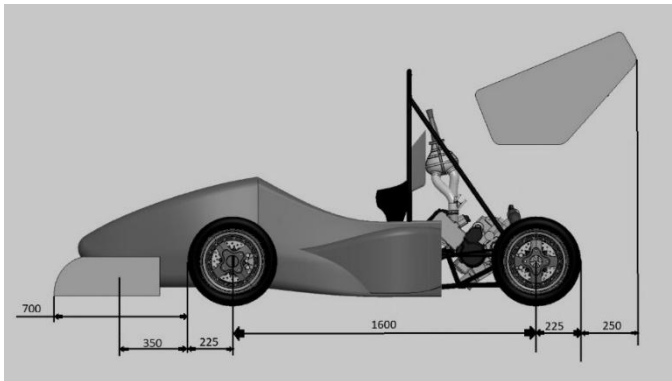
Fig. 8. Side view of the prototype along with its dimensions

Upon balancing the moments about the COG of the prototype, (F_D is assumed to be the downforce expected by the rear wing)

$$\left(\frac{700}{2} + 255 + \frac{1600}{2}\right)(163.69) = \left(\frac{1600}{2} + 255 + \frac{250}{2}\right)(F_D)$$

$$F_D = 194.90\text{N}$$

3.2 Rear wing

After the moment balancing, multiple iterations are performed to get the desired result. It's easier to make changes to get various results by changing chord length, angle of attack and number of wings. As the rear wing is well above ground, ground effect doesn't play a major role in the same. Table 8 and 9

represents the report of drag force and down force for rear wing obtained from ANSYS Fluent. It can be seen that a down force of 177.73 N and a drag of 51.76 N was developed on rear wing.

Table 7. Result report of down force and drag force from ANSYS Fluent for rear wing

Zone	Down Force (N)	Drag Force (N)
Wall-enclosure	177.73235	51.76918
Net	177.73235	51.76918

Hence the total downforce from front and rear wing was found to be

Front wing downforce + Rear wing downforce = 163.69 + 177.73

$$\text{Total downforce} = 341.42N$$
$$= 34.8kgf$$

The total drag from front and rear wings was found to be

Front wing downforce + Rear wing downforce = 29.83 + 51.76

$$\text{Total drag} = 81.59N$$
$$= 8.317 \text{ kgf}$$

4.0 Conclusion

Design and development of front and rear wing for an existing FSAE prototype car was carried out successfully. ANSYS Fluent simulations were carried out with different aerofoils and different configurations to achieve the desired down force of around 30 kgf without much increase in drag force at Reynolds number 1.84×10^5. S1223 front and rear wing element was successful in achieving a down force of 34.8 kgf with a drag force of 8.317kgf.

References

1. R G Dominy Aerodynamics of Grand Prix Cars, *Journal of Automobile Engineering*, 206(4). 267-274, 1992
2. S S Pakkam, High Downforce Aerodynamics for Motorsports, *Master's Thesis*, North Carolina State University, 2011
3. A J Peters, N Moore and P A Wilson - An investigation into wing in ground effect airfoil geometry, *Proceedings of the Symposium on Challenges in Dynamics, System Identification, Control and Handling Qualities for Land, Air and Sea Vehicles*, Paris, France, 11-20, 2002
4. H. Al- Kayiem and K Chelven, An Investigation on the Aerodynamic Characteristics of a 2-D Airfoil in Ground Collision*, Journal of Engineering Science and Technology*, 6 (3), 369-381, 2011

5. S Wordley, J Saunders, Aerodynamics for Formula SAE: Initial design and performance prediction, *Proceedings of the SAE World Congress and Exhibition, Detroit, U.S.A*, 8-20, 2006
6. H Dahlberg, Aerodynamic Development of Formula Student Race Car *Master's Thesis*, KTH Mechanics University, 2007
7. J Zerihan and X Zhang, Aerodynamics of a Single Element Wing in Ground Effect, *Journal of Aircraft*, 37 (6), 2000